INSTITUTE OF PHYSICS PUBLISHING EUROPEAN JOURNAL OF PHYSICS

Eur. J. Phys. **25** (2004) 535–554 PII: S0143-0807(04)76708-2

Parametric excitation of a linear oscillator

Eugene I Butikov

St Petersburg State University, St Petersburg, Russia

E-mail: butikov@spb.runnet.ru

Received 25 February 2004
Published 28 May 2004
Online at stacks.iop.org/EJP/25/535
DOI: 10.1088/0143-0807/25/4/009

Abstract

The phenomenon of parametric resonance is explained and investigated both analytically and with the help of a computer simulation. Parametric excitation is studied for the example of the rotary oscillations of a simple linear system—mechanical torsion spring pendulum excited by periodic variations of its moment of inertia. Conditions and characteristics of parametric resonance and regeneration are found and discussed in detail. Ranges of frequencies within which parametric excitation is possible are determined. Stationary oscillations at the boundaries of these ranges are investigated. The simulation experiments aid greatly an understanding of basic principles and peculiarities of parametric excitation and complement the analytical study of the subject in a manner that is mutually reinforcing.

1. Introduction: the investigated physical system

A physical system undergoes a parametric forcing if one of its parameters is modulated periodically with time. A common familiar example of parametric excitation of oscillations is given by the playground swing on which most people have played in childhood (see, e.g., [1]). The swing can be treated as a physical pendulum whose reduced length changes periodically as the child squats at the extreme points, and straightens when the swing passes through the equilibrium position. It is easy to illustrate this phenomenon in the classroom with the following simple experiment. Let a thread with a bob hanging from its one end pass through a little ring fixed in a support. You can pull by some small length the other end of the thread that you are holding in your hand each time the swinging bob passes through the middle position and release the thread to its previous length each time the bob reaches the maximum deflection. These periodic variations of the pendulum length with the frequency twice the frequency of natural oscillation cause the amplitude to increase progressively. Another canonical example of parametric pumping is given by a pendulum whose support oscillates vertically (see [2]).

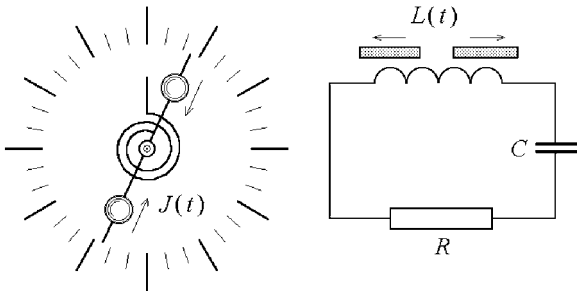

Figure 1. Schematic image of the torsion spring oscillator with a balanced rotor whose moment of inertia is forced to vary periodically (left), and an analogous *LCR*-circuit with a coil whose inductance is modulated (right).

However, such systems do not perfectly suit the initial acquaintance with parametric excitation because the ordinary pendulum is a *nonlinear* physical system: the restoring torque of the gravitational force is proportional to the sine of the deflection angle. That is why we suggest studying the basics of parametric resonance by using the simplest *linear* mechanical system in which the phenomenon is possible, namely, the torsion spring oscillator, similar to the balance device of a mechanical watch. An educational computer program that simulates such a system has been developed by the author (see [3]).

The left-hand side of figure 1 shows a schematic image of the apparatus. It consists of a rigid rod which can rotate about an axis that passes through its centre. Two identical weights are balanced on the rod. An elastic spiral spring is attached to the rod. The other end of the spring is fixed. When the rod is turned about its axis, the spring flexes. The restoring torque $-D\varphi$ of the spring is proportional to the angular displacement φ of the rotor from the equilibrium position. After a disturbance, the rotor executes a harmonic torsional oscillation.

To provide modulation of a system parameter, we assume that the weights can be shifted simultaneously along the rod in opposite directions to other symmetrical positions so that the rotor as a whole remains balanced. However, its moment of inertia J is changed by such displacements of the weights. When the weights are shifted towards or away from the axis, the moment of inertia decreases or increases, respectively. Thus, the moment of inertia of the rotor is the parameter to be modulated in the investigated physical system. As the moment of inertia J is changed, so also is the natural frequency $\omega_0 = \sqrt{D/J}$ of the torsional oscillations of the rotor. Periodic modulation of the moment of inertia can cause, under certain conditions, a growth of (initially small) natural rotary oscillations of the rod.

This physical system, being useless for any practical application, is nevertheless ideal for gaining conceptual knowledge about the basics of parametric resonance and has several advantages in an educational context because it gives a very clear example of the phenomenon in a *linear* mechanical system. All peculiarities of parametric excitation in this linear system can be completely explained and exhaustively investigated by modest means even quantitatively.

Parametric excitation is also possible in an electromagnetic analogue of the spring oscillator, namely in a series *LCR*-circuit containing a capacitor, an inductor (a coil) and a resistor (right-hand side of figure 1). An oscillating current in the circuit can be excited by periodic changes in the capacitance if we periodically move the plates closer together and farther apart, or by changes in the inductance of the coil if we periodically move an iron core in and out of the coil. Such periodic changes in the inductance are quite similar to the changes in the moment of inertia in the mechanical system considered above. However, the

mechanical system has certain spectacular didactic advantages primarily because its motion is easily represented on the computer screen, and it is possible to see directly what is happening [3]. Such a visualization makes the simulation experiments very convincing and easy to understand, aiding a great deal in developing our physical intuition.

2. Peculiarities of parametric resonance

The causes and characteristics of parametric resonance are considerably different from those of the resonance occurring when the oscillator responds to a periodic external force exerted directly on the system. Specifically, the resonant relationship between the frequency of modulation of a parameter and the mean natural frequency of oscillation of the system is different from the relationship between the driving frequency and the natural frequency for the usual resonance in forced oscillations. Parametric excitation can occur only if at least weak natural oscillations already exist in the system, and if there is friction, the amplitude of modulation of the parameter must exceed a certain threshold value in order to cause parametric resonance.

To understand how a change in the moment of inertia can increase or decrease the angular velocity of the rotor, let us imagine for a while that the spiral spring is absent. Then the angular momentum of the system would remain constant as the weights are being moved along the rod. Thus the resulting reduction in the moment of inertia is accompanied by an increment in the angular velocity, and the rotor acquires additional energy. The system is similar in some sense to a spinning figure skater, whose rotation accelerates as she moves her initially stretched arms closer to her body.

The greater the initial angular velocity, the greater the increment in the velocity and the energy. This additional energy is supplied to the rotor by the source that moves the weights along the rod. On the other hand, if the weights are moved apart along the rotating rod, the angular velocity and the energy of the rotor diminish. The decrease in energy is transmitted back to the source.

In order that increments in energy occur regularly and exceed the amounts of energy returned, i.e., in order that, as a whole, the modulation of the moment of inertia regularly feeds the oscillator with energy, the period and the phase of modulation must satisfy certain conditions. Figure 2 shows the graphs of parametric oscillations of the torsion pendulum excited by a constrained sinusoidal motion of the weights along the rod with a period which is equal to one-half of the natural period. The graphs are obtained with the help of a computer simulation program included in the educational software package [3].

To provide a growth of energy by modulation of the moment of inertia, the motion of the weights towards the axis of rotation must occur while the angular velocity of the rotor is on average greater in magnitude than it is when the weights are moved apart to the ends of the rod. The graphs in figure 2 correspond to this case: we see clearly that during the intervals of negative values of v, the angular velocity $\dot{\varphi}$ is greater in magnitude than during the intervals of positive v. Otherwise the modulation of the moment of inertia aids the damping of the natural oscillations.

Parametric excitation is possible only if one of the energy-storing parameters, D or J (C or L in the case of a LCR-circuit), is modulated. Modulation of the resistance R (or of the damping constant γ in the mechanical system) can affect only the character of the damping of oscillations. It cannot generate an increase in their amplitude.

The strongest parametric oscillations are excited when the cycle of modulation is repeated twice during one period T_0 of natural oscillations in the system, i.e., when the frequency ω of parametric modulation is twice the natural frequency ω_0 of the system. But the delivery

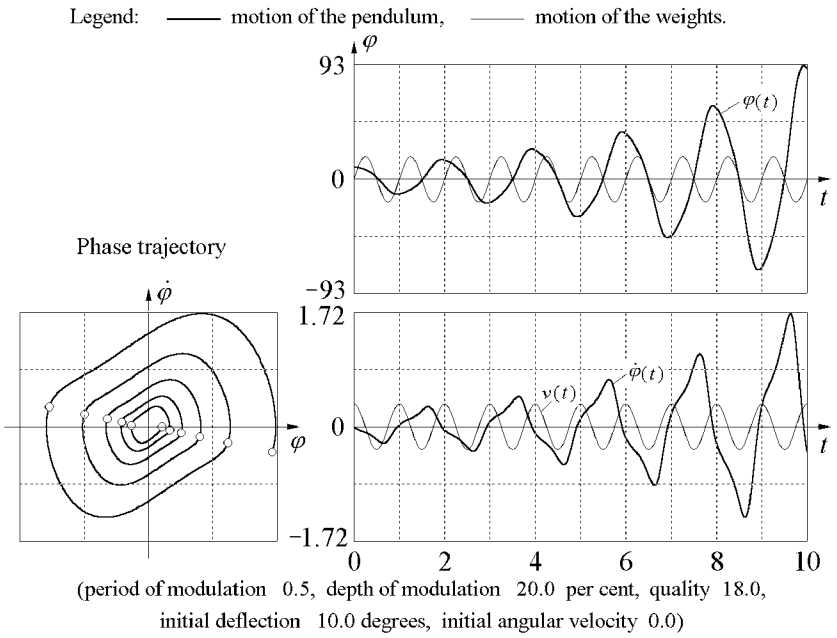

Figure 2. Graphs of the angular displacement and velocity of the rotor and the phase trajectory in conditions of the principal parametric resonance.

of energy is also possible when the parameter changes once during one period, twice during three periods and so on. That is, parametric resonance is possible when one of the following conditions for the frequency ω of modulation (or for the period of modulation $T = 2\pi/\omega$) is fulfilled:

$$\omega = 2\omega_0/n, \qquad T = nT_0/2, \tag{1}$$

where $n = 1, 2, \ldots$. For a given amplitude of modulation of the parameter, the higher the order n of parametric resonance, the less (in general) the amount of energy delivered to the oscillating system during one period.

One of the most interesting characteristics of parametric resonance is the possibility of exciting increasing oscillations not only at the frequencies ω_n given in equation (1), but also in intervals of frequencies lying on either side of the values ω_n (in the *ranges of instability*.) These intervals become wider as the range of parametric variation is extended, that is, as the depth of modulation is increased.

An important distinction between parametric excitation and forced oscillations is related to the dependence of the growth of energy on the energy already stored in the system. While for a direct forced excitation, the increment of energy during one period is proportional to the *amplitude* of oscillations, i.e., to the square root of the energy, at parametric resonance the increment of energy is proportional to the *energy* stored in the system.

Energy losses caused by friction (unavoidable in any real system) are also proportional to the energy already stored. In the case of direct forced excitation, an arbitrarily small external force gives rise to resonance. However, energy losses restrict the growth of the amplitude because these losses increase with the energy faster than does the investment of energy arising from the work done by the external force.

In the case of parametric resonance, both the investment of energy caused by the modulation of a parameter and the frictional losses are proportional to the energy stored

(to the square of the amplitude), and so their ratio does not depend on the amplitude. Therefore, parametric resonance is possible only when a *threshold* is exceeded, that is, when the increment of energy during a period (caused by the parametric variation) is larger than the amount of energy dissipated during the same time. To satisfy this requirement, the range of the parametric variation (the depth of modulation) must exceed some critical value. This threshold value of the depth of modulation depends on friction. However, if the threshold is exceeded, the frictional losses of energy cannot restrict the growth of the amplitude. In a linear system the amplitude of parametrically excited oscillations must grow indefinitely.

In a nonlinear system the natural period depends on the amplitude of oscillations. If conditions for parametric resonance are fulfilled at small oscillations and the amplitude begins to grow, the conditions of resonance become violated at large amplitudes. In a real system the growth of the amplitude over the threshold is restricted by nonlinear effects.

3. Parametric resonance and the threshold of parametric excitation

To explain the behaviour of the parametrically pumped oscillator, first we make use of the conservation of energy. At resonance, additional energy must be transmitted to the rotor by the source that makes the weights move periodically along the rod. Therefore, we calculate the work done by the source during one period of oscillation and find those conditions under which this work is positive.

In this model we assume the forced motion of the weights along the rod to be exactly sinusoidal, and so their distance l from the axis of rotation varies with time according to the following expression:

$$l(t) = l_0(1 + m\sin\omega t). \tag{2}$$

Here l_0 is the mean distance of the weights from the axis of rotation, and m is the dimensionless (fractional) amplitude of their harmonic motion along the rod ($m < 1$). For simplicity, we let the rod be very light compared to the weights. We note that m is the modulation depth of the distance $l(t)$, while the modulation depth m_J of the moment of inertia $J(t)$ is approximately twice as great ($m_J \approx 2m$ if $m \ll 1$), because the moment of inertia is proportional to the square of the distance of the weights from the axis of rotation.

From equation (2), we find that a weight moves along the rod with a velocity and acceleration (relative to the rod) which change with time as $\cos\omega t$ and $-\sin\omega t$, respectively:

$$v(t) = \mathrm{d}l/\mathrm{d}t = \omega l_0 m\cos\omega t, \qquad a_r(t) = \mathrm{d}v/\mathrm{d}t = -\omega^2 l_0 m\sin\omega t. \tag{3}$$

In order to find the force F exerted on the weight by the device that makes it move along the rod, we use a noninertial reference frame rotating with the rod. Applying Newton's second law to the motion of the weight in this rotating frame of reference, we must take into account the centrifugal pseudo force of inertia exerted on the weight, $M\dot{\varphi}^2(t)l(t)$, where M is the mass of the weight and $\dot{\varphi}(t)$ is the angular velocity of the rod:

$$Ma_r(t) = F(t) + M\dot{\varphi}^2(t)l(t). \tag{4}$$

We are interested in the work of this force $F(t)$ done during one period of oscillation. The amount of this work (for both weights) equals the change in the energy of oscillations during one period. For the infinitesimal element of work $\mathrm{d}W$ done during a time interval $\mathrm{d}t$ (during which the weight is displaced along the rod a distance $\mathrm{d}l = v(t)\,\mathrm{d}t$), we can write

$$\mathrm{d}W = F(t)\,\mathrm{d}l = F(t)v(t)\,\mathrm{d}t = [Ma_r(t) - M\dot{\varphi}^2(t)l(t)]v(t)\,\mathrm{d}t. \tag{5}$$

As we see from equation (3), the radial velocity $v(t)$ of the weight in equation (5) is proportional to the dimensionless amplitude m of its forced motion along the rod. If we

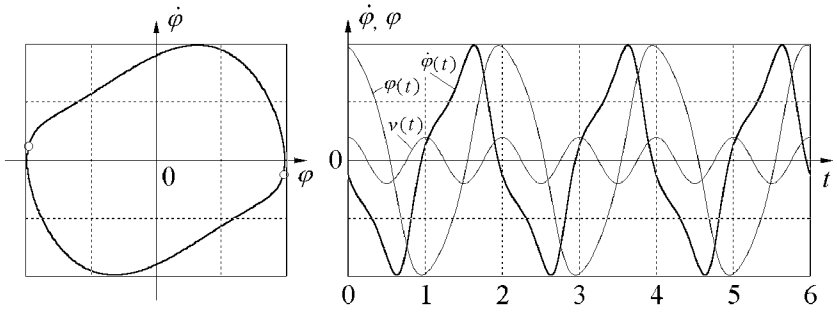

Figure 3. The phase trajectory of stationary oscillations at the threshold conditions (the mode of parametric regeneration at $m \approx 1/Q$), and the time-dependent graphs of the rotor angular velocity and of the radial velocity of the weights.

restrict our calculations to the first order of the small parameter m, we need to keep only the second term in square brackets in equation (5), and we can substitute for $l(t)$ from equation (2) only its mean value l_0:

$$\mathrm{d}W \approx -M\dot\varphi^2(t) l_0 v(t)\,\mathrm{d}t = -M\dot\varphi^2(t) l_0^2 \omega m \cos\omega t. \tag{6}$$

As we noted above, the most favourable condition for the parametric excitation of the rotor occurs if the weights execute two full cycles of the forced motion during one mean period of the natural oscillation. In other words, the frequency ω in equations (2) and (6) must be approximately twice the mean natural frequency $\omega_0 = 2\pi/T_0$ of oscillation of the rotor. (Here ω_0 is the frequency of free oscillations of the rotor with the weights fixed at their average distance l_0 from the axis). For small values of the dimensionless amplitude m, the frequency of modulation $\omega = 2\omega_0$ in equation (2) corresponds to exact tuning to the principal resonance ($n = 1$).

In addition, it is necessary that a certain phase relation between the forced motion of the weights and the torsional oscillations of the rotor be satisfied: namely, the weights must move with maximal relative velocity towards the axis of rotation at moments when the oscillating rod moves with its greatest angular velocity. This phase relation is satisfied for the motion of the weights described by equations (2) and (3) provided we assume the following time dependence for the torsional oscillations of the rotor:

$$\varphi(t) = \varphi_m \cos\omega_0 t, \qquad \dot\varphi(t) = -\varphi_m \omega_0 \sin\omega_0 t. \tag{7}$$

These are only approximate expressions because, strictly speaking, the torsional oscillation of the rotor is not harmonic (see figure 3). Deviations from a sinusoidal oscillation are caused by the motion of the weights since this motion influences the moment of inertia and hence the angular velocity of the rotor.

After the substitution of $\omega = 2\omega_0$ and $\dot\varphi(t)$ from equation (7) into equation (6), we can integrate $\mathrm{d}W$ given by (6) over a period $T_0 = 2\pi/\omega_0$, taking into account that the mean value of $\cos^2\omega_0 t$ is $1/2$. Finally we find that (up to terms of the first order in the small value m), the work W of the force $F(t)$ done during a period T_0 is given by the following expression:

$$W = \tfrac{1}{2} M \varphi_m^2 \omega_0^2 l_0^2 \cdot 2\pi m. \tag{8}$$

The same expression is valid for the second weight, and so as a whole the forces exerted on the weights perform positive work ($W > 0$) during a period and increase the energy of the oscillator by the amount $2W$:

$$\Delta E = 2W = M\varphi_m^2\omega_0^2 l_0^2 \cdot 2\pi m. \tag{9}$$

Since we assume the rod to be very light compared to the weights, we can consider the total kinetic energy of the rotor to be the kinetic energy of these massive weights. The total energy E of the oscillator is equal to the maximal value of its kinetic energy, which is attained at the instants when the oscillating rotor moves near its equilibrium position and has its greatest angular velocity $\omega_0\varphi_m$. Therefore $E = M\varphi_m^2\omega_0^2 l_0^2$. We do not take into account here the kinetic energy of the weights in their radial motion along the rod, because this energy is proportional to the square of small parameter m. Comparing this expression with the right-hand side of equation (9), we see the most essential feature of parametric resonance, namely that the investment of energy ΔE due to modulation of a parameter is proportional to the energy E already stored in the oscillator:

$$\Delta E = 2\pi m E. \tag{10}$$

Equation (10) means that at parametric resonance the total energy E of oscillations, averaged over a period $T_0 = 2\pi/\omega_0$ of oscillation, grows exponentially with time:

$$\frac{\mathrm{d}E}{\mathrm{d}t} = m\omega_0 E, \qquad E(t) = E_0 \exp(2\alpha t), \qquad \text{where} \quad 2\alpha = m\omega_0. \tag{11}$$

This result is valid in the absence of friction. Dissipation of the mean energy E due to viscous friction is also described by an exponential function:

$$\frac{\mathrm{d}E}{\mathrm{d}t} = -2\gamma E, \qquad E(t) = E_0 \exp(-2\gamma t). \tag{12}$$

At the threshold of parametric resonance, these energy losses are just compensated for by the delivery of energy arising from the forced periodic motion of the weights. In this instance, $\gamma = \alpha$. Thus we can find the minimal value of m (for a given value of γ or of the quality factor Q) which makes parametric excitation possible:

$$m_{\min} = \frac{2\gamma}{\omega_0} = \frac{1}{Q}. \tag{13}$$

Equivalently, the threshold condition can be expressed in terms of the maximal value of the damping constant γ (or the minimal quality factor Q) for a given value m of the amplitude in (2):

$$\gamma_{\max} = \frac{1}{2}m\omega_0, \qquad Q_{\min} = \frac{\omega_0}{2\gamma_{\max}} = \frac{1}{m}. \tag{14}$$

These results concerning the threshold of parametric excitation are approximate and are valid only for small values of the dimensionless amplitude m of the forced motion of the weights along the rod. The simulation program [3] executes numerical integration of the differential equation of motion. This integration is not restricted to small values of m. Thus the simulation allows us to find the threshold conditions experimentally (by trial and error) with greater accuracy.

Steady oscillations occurring at the threshold are called *parametric regeneration*. They are shown in figure 3. These graphs should be compared with those shown in figure 2, which displays plots of resonant oscillations occurring above the threshold, where the amplitude grows exponentially in spite of the friction.

When the depth of modulation exceeds the threshold value, the (averaged over the period) energy of oscillations increases exponentially with time. The growth of the energy again is

described by equation (11). However, now the index of growth 2α is determined by the amount by which the energy delivered through parametric modulation exceeds the simultaneous losses of energy caused by friction: $2\alpha = m\omega_0 - 2\gamma$. The energy of oscillations is proportional to the square of the amplitude. Therefore, the amplitude of parametrically excited oscillations also increases exponentially with time (see figure 2): $a(t) = a_0 \exp(\alpha t)$ with the index α (one-half the index 2α of the growth in energy). For the principal resonance we have $\alpha = m\omega_0/2 - \gamma$.

4. Differential equation for sinusoidal motion of the weights

In the assumed model, we consider the rod itself to be very light, so that the moment of inertia J of the rotor is due principally to the weights: $J = 2Ml^2(t)$. The angular momentum $J\dot{\varphi}(t)$ changes with time according to the equation:

$$\frac{\mathrm{d}}{\mathrm{d}t}(J\dot{\varphi}) = -D\varphi, \tag{15}$$

where $-D\varphi$ is the restoring torque of the spring. Substituting into equation (15) $l(t)$ from equation (2) and taking into account that $\omega_0^2 = D/J_0$ ($J_0 = 2Ml_0^2$ is the moment of inertia with the weights in their mean positions), we obtain finally:

$$\frac{\mathrm{d}}{\mathrm{d}t}[(1 + m\sin\omega t)^2\dot{\varphi}] = -\omega_0^2\varphi - 2\gamma\dot{\varphi}. \tag{16}$$

We have added the drag torque of viscous friction to the right-hand side of equation (16). This equation is solved numerically in the computer program [3] in real time during the simulation.

We note that the harmonic motion of the weights along the rod described by equation (2) does not mean that the moment of inertia $J(t)$ is harmonically modulated. Indeed, J is proportional to the *square* of the distance $l(t)$ rather than to its first power. The time dependence of $J(t)$ includes the second harmonic of the frequency ω. Only for small values of the amplitude m (when $m \ll 1$) can we consider the modulation of the moment of inertia to be approximately sinusoidal:

$$J(t) = 2Ml^2(t) = 2Ml_0^2(1 + m\sin\omega t)^2 \approx 2Ml_0^2(1 + 2m\sin\omega t) = J_0(1 + m_J\sin\omega t), \tag{17}$$

where $J_0 = 2Ml_0^2$ is the mean value of the moment of inertia, and $m_J = 2m$ is the depth of its modulation. (We note that the value of m_J is approximately twice the value of m.) If we are interested only in an approximate solution valid up to terms of the first order in the small parameter m, then instead of the exact differential equation of motion, equation (16), we can solve the following approximate equation:

$$\ddot{\varphi} + 2\gamma\dot{\varphi} + \omega_0^2(1 - 2m\sin\omega t)\varphi = 0. \tag{18}$$

We ignore here the modulation of the coefficient of $\dot{\varphi}$ because for parametric resonance, the variation of only those parameters which store energy (the moment of inertia and the torsion spring constant) is essential. Modulation of the damping constant γ cannot excite oscillations.

When $\gamma = 0$, equation (18) is called *Mathieu's equation*. The theory of Mathieu's equation has been fully developed, and all significant properties of its solutions are well known (see, for example, [4]). A complete mathematical analysis of Mathieu's equation is rather complicated and gives little insight into the physics of parametric excitation. This analysis is usually restricted to the determination of the frequency intervals within which the state of rest in the equilibrium position becomes unstable, so that at arbitrarily small deviations from the state of rest the amplitude of incipient small oscillations increases progressively with time. The boundaries of these *intervals of instability* depend on the depth of modulation m.

We emphasize that the application of the theory of Mathieu's equation to the simulated system is restricted to the linear order in m. For finite values of the depth of modulation m, the resonant frequencies and the boundaries of the intervals of instability for the simulated system differ from those predicted by Mathieu's equation. We shall see this point in the following section, in which we avoid struggling with Mathieu's equation or Floquet theory and develop a rather simple theory of the simulated system up to the terms of the second order in m by using the approach described in [5].

5. The principal interval of parametric instability

In the vicinity of the principal resonance, the frequency of modulation is approximately twice the natural frequency ($\omega \approx 2\omega_0$), and we can express ω in the form $\omega = 2\omega_0 + \varepsilon$, where ε is a small detuning from resonance ($|\varepsilon| \ll \omega_0$). We then propose that an approximate solution $\varphi(t)$ to equation (16) represents a nearly harmonic motion with the frequency $\tilde{\omega} = \omega/2 = \omega_0 + \varepsilon/2$. We let the amplitude and phase of the trial function $\varphi(t)$ slowly vary with time:

$$\varphi(t) = p(t)\cos\tilde{\omega}t + q(t)\sin\tilde{\omega}t. \tag{19}$$

Here $p(t)$ and $q(t)$ are functions of time that vary slowly relative to the oscillating sine and cosine functions. In the exact solution to equation (16) there are also higher harmonics with the frequencies $3\tilde{\omega}, 5\tilde{\omega}, \ldots$, but their contribution is proportional to higher powers of the small parameter $m \ll 1$. We do not include these higher harmonics in the approximate solution expressed by equation (19).

The time variation of the amplitudes $p(t)$ and $q(t)$ is caused by the modulation of the moment of inertia, and so the time derivatives of functions $p(t)$ and $q(t)$ are also proportional to the small quantity m. Substituting φ from equation (19) into the differential equation, equation (16), we can express the products of the sine and cosine functions in the following way:

$$\sin 2\tilde{\omega}t\cos\tilde{\omega}t = (\sin\tilde{\omega}t + \sin 3\tilde{\omega}t)/2, \qquad \sin 2\tilde{\omega}t\sin\tilde{\omega}t = (\cos\tilde{\omega}t - \cos 3\tilde{\omega}t)/2,$$

and omit in the equation the higher harmonics with the frequency $3\tilde{\omega}$. Thus for the unknown functions $p(t)$ and $q(t)$ we obtain the following system of differential equations of the first order:

$$\begin{aligned} &2\tilde{\omega}\dot{q} - \left(\tilde{\omega}^2 - \omega_0^2\right)p + \left(2\gamma\tilde{\omega} - m\omega_0^2\right)q = 0, \\ &-2\tilde{\omega}\dot{p} - \left(2\gamma\tilde{\omega} + m\omega_0^2\right)p - \left(\tilde{\omega}^2 - \omega_0^2\right)q = 0. \end{aligned} \tag{20}$$

We have omitted here the terms $2\gamma\dot{p}$ and $2\gamma\dot{q}$ since parametric excitation is possible only if friction is small enough (from equation (14) we see that $2\gamma < m\omega_0$). The contribution of these omitted terms to equation (20) is of the order m^2.

According to general rules, we can search for a solution to these equations in the form $\exp\alpha t$. The condition for the existence of a nontrivial (nonzero) solution to this system of homogeneous equations gives the following expression for α:

$$\alpha \approx \tfrac{1}{2}\sqrt{(m\omega_0)^2 - \varepsilon^2} - \gamma. \tag{21}$$

Here we have taken into account that $\tilde{\omega}^2 \approx \omega_0^2 + \omega_0\varepsilon$. If there is an exact tuning to resonance, the deviation in frequency ε vanishes ($\varepsilon = 0$), and equation (21) gives the following value for the index α that determines the exponential growth in the amplitude of parametrically excited oscillations:

$$\alpha \approx m\omega_0/2 - \gamma. \tag{22}$$

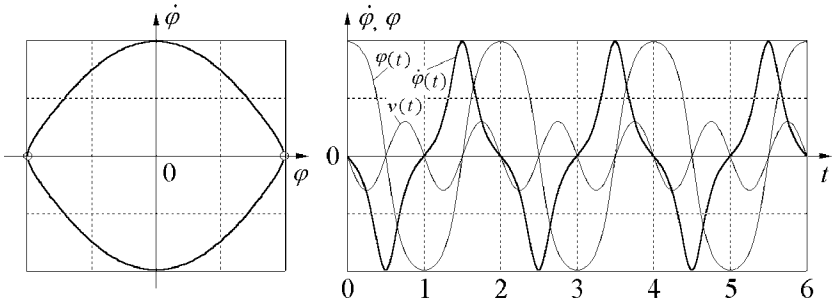

Figure 4. The phase trajectory of stationary oscillations occurring at the left boundary of the principal instability interval (left), and the time-dependent graphs of the angular velocity and of the radial velocity of the weights (right).

The amplitude of oscillation grows if $\alpha > 0$. Therefore, for the threshold of parametric resonance we obtain $m = 2\gamma/\omega_0 = 1/Q$. The same value for the threshold of parametric excitation under conditions of exact tuning to resonance is obtained above by using the conservation of energy (see equation (13)). For zero friction, the index of the exponential resonant growth in the amplitude is proportional to the depth of modulation: $\alpha = m\omega_0/2$.

For the case in which friction is absent ($\gamma = 0$), and for a given value m of the depth of modulation, we find from equation (21) that the linearized differential equation, equation (16), yields resonant solutions (i.e. solutions whose amplitude is growing with time) if the frequency of modulation belongs to some interval which extends by $\Delta\omega$ on either side of the resonant value $\omega_{\rm res} = 2\omega_0$. The half-width of the interval $\Delta\omega = m\omega_0$ is proportional to the amplitude m of the forced oscillation of the weights. For a value ω of the frequency of modulation lying somewhere within the interval, the amplitude of parametrically excited oscillations grows exponentially with time as $\exp(\alpha t)$, where the index α of the growth is given by equation (21) with $\gamma = 0$:

$$\alpha = \tfrac{1}{2}\sqrt{(m\omega_0)^2 - (\omega - \omega_{\rm res})^2}. \tag{23}$$

(for $|\omega - \omega_{\rm res}| \leqslant m\omega_0$). The value of α is zero at the boundaries $\omega_\pm$ of the interval of instability: $\omega_\pm = \omega_{\rm res} \pm m\omega_0$. At these boundaries, stationary oscillations of a constant amplitude are possible. An example of such oscillations is shown in figure 4.

The symmetric shape of these graphs shows clearly that on average there is no energy transfer to the frictionless oscillator: the energy gained during one-half-cycle of modulation is returned back during the next half-cycle.

In order to obtain more precise values for the frequencies of modulation $\omega_\pm$ which correspond to the boundaries of the instability interval, we need to include higher harmonics in the trial function $\varphi(t)$ for an approximate solution of equation (16). Their frequency $3\tilde\omega, 5\tilde\omega, \ldots$ is an odd-number multiple of the fundamental frequency $\tilde\omega = \omega/2 \approx \omega_0$. Restricting the calculation up to the second order in m, we hold only the first and third harmonics in the trial function:

$$\varphi(t) = C_1 \cos\tilde\omega t + S_1 \sin\tilde\omega t + C_3 \cos 3\tilde\omega t + S_3 \sin 3\tilde\omega t. \tag{24}$$

If we are interested only in the boundaries $\omega_\pm$ of the interval of instability, at which the oscillations are stationary and their amplitude does not vary with time, we can assume the coefficients C_1, S_1, C_3 and S_3 to be constant.

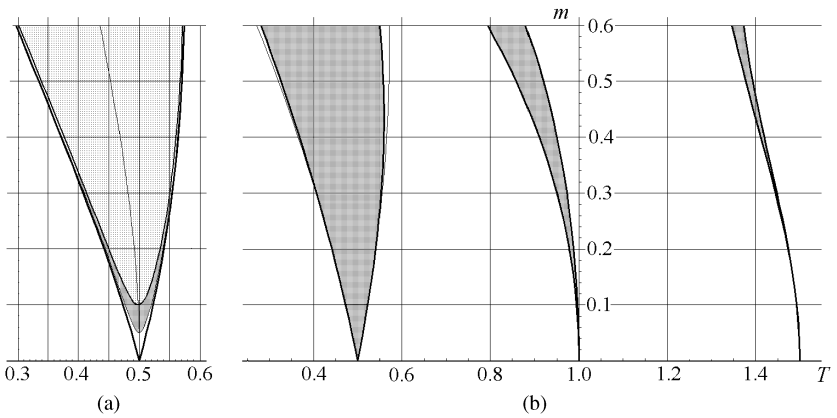

Figure 5. Principal instability interval (a) and the diagram showing the boundaries of the first three intervals (b). Thin curves which deviate slightly at large m values from the boundaries of the principal interval are plotted according to the approximate expression (25).

Substituting equation (24) into equation (16), we can omit the terms with frequency $5\tilde{\omega}$. In the terms with frequency $\tilde{\omega}$ we need to keep quantities up to the first and second order in m, while in the terms with frequency $3\tilde{\omega}$ we need to keep only the terms of the first order. Finally we arrive at a system of homogeneous equations for C_1, S_1, and C_3, S_3. The condition for the existence of a nontrivial solution to the system gives us approximate expressions for the desired boundaries $\omega_\pm$:

$$\omega_\pm = 2\omega_0\bigl(1 \pm \tfrac{1}{2}\sqrt{m^2 - (1/Q)^2} + \tfrac{11}{16}m^2\bigr). \tag{25}$$

The term of the second order in m has the same value for both boundaries of the interval. It does not influence the width of the interval, shifting it as a whole by a value proportional to m^2.

The structure of the principal interval of parametric instability is shown in figure 5(a) for the absence of friction (thick bounding curves), for $Q = 20$, and $Q = 10$ (thin inner curves). It is more convenient to express the boundaries using not the frequency ω of the parametric modulation, but rather the period $T = 2\pi/\omega$. This convention is usually used in presenting the stability map for Mathieu-type systems by the so-called Incze–Strutt diagrams. We also use it in the simulation program [3] and for all figures in this paper. The shaded regions in figure 5(b) show the first three intervals of parametric instability in one T–m diagram[1].

In the presence of viscous friction the principal interval reduces as the friction is increased and disappears if $Q < 1/m$: its boundaries merge at the threshold. Equation (25) gives, for the threshold, the value $m_{\min} = 1/Q$ which has been found above, equation (13), from considerations based on the energy conservation.

An example of steady oscillations occurring at the left boundary of the principal instability interval is shown in figure 4. The upper part of figure 6 shows the phase diagram and the graphs of steady oscillations at the right boundary of the interval in the absence of friction. We note the departure of the shape of these graphs from a sine curve, which is caused by the contribution of higher harmonics (mainly of the third harmonic with the frequency $3\tilde{\omega} = \frac{3}{2}\omega$). The ratio of the amplitude of the third harmonic to the amplitude of the fundamental harmonic is approximately the same for both boundaries $\bigl(|C_3/C_1| \approx \frac{3}{8}m\bigr)$. The difference in the

[1] Actually the curves in figure 5 are plotted with the help of somewhat more complicated formulae than equation (25) (not cited in this paper), which are obtained by holding several harmonic components in the trial function $\varphi(t)$.

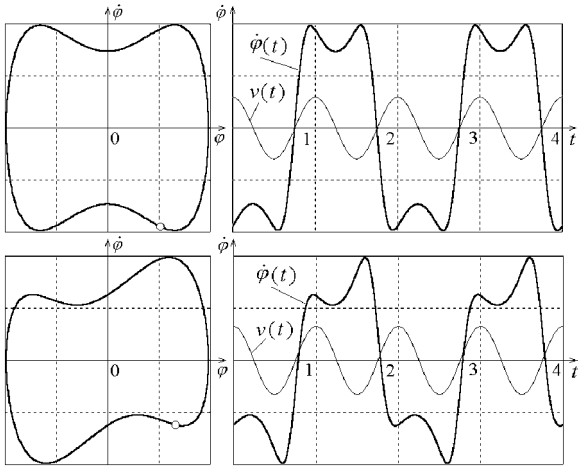

Figure 6. The phase trajectory of stationary oscillations occurring at the right boundary of the principal instability interval (left), and the time-dependent graphs of the angular velocity of the rotor and of the radial velocity of the weights (right).

patterns of oscillations at the left and right boundaries (compare the graphs in figures 4 and 6) is explained by the different phase shift of the third harmonic with respect to the fundamental one.

The lower part of figure 6 corresponds to the right boundary in the presence of friction. From the asymmetry of the graph, it is clear that in this case the energy received by the oscillator is greater than the energy returned: during the intervals of negative values of v (while the weights are moving towards the axis) the angular velocity $\dot\varphi$ is greater in magnitude. The energy excess compensates for the frictional losses, providing the stationary oscillations. Outside the instability interval, the modulation of the moment of inertia causes only a few changes in the shape of those decaying natural oscillations which may have been excited.

The simulations show that stationary oscillations at the boundaries of the principal resonance include also the fifth and even seventh harmonic components with frequencies $\frac{5}{2}\omega$ and $\frac{7}{2}\omega$, respectively. To find the boundaries with greater precision, we should include these high harmonics into the trial function $\varphi(t)$, equation (24). For the frictionless oscillator it is more convenient to choose the time origin in such a way that the motion of the weights along the rod is described in equation (2) by $l(t) = l_0(1 + m\cos\omega t)$ instead of the sine function. In this case the sine and cosine harmonics do not mix, that is, the stationary oscillations at the left boundary of the interval include only harmonics of the cosine type, and at the right boundary—of the sine type.

The final analytical expressions for the frequencies (and periods) of modulation and for the relative contributions of high harmonics (as functions of m) at the boundaries of the instability interval are complicated and hence not cited in this paper. However, they show a very good agreement with the simulations. We cite here the calculated values for a certain modulation depth $m = 0.3$ (30%). The corresponding experimental values (obtained in the simulation) are shown in parentheses:

- Left (cosine-type) boundary: period $T/T_0 = 0.4066$ (0.4066);
  $C_3/C_1 = -0.103$ (-0.101); $C_5/C_1 = 0.015$ (0.016); $C_7/C_1 = 0.002$ (0.001).
- Right (sine-type) boundary: period $T/T_0 = 0.5528$ (0.5528);
  $S_3/S_1 = -0.129$ (-0.129); $S_5/S_1 = 0.020$ (0.020); $S_7/S_1 = 0.003$ (0.003).

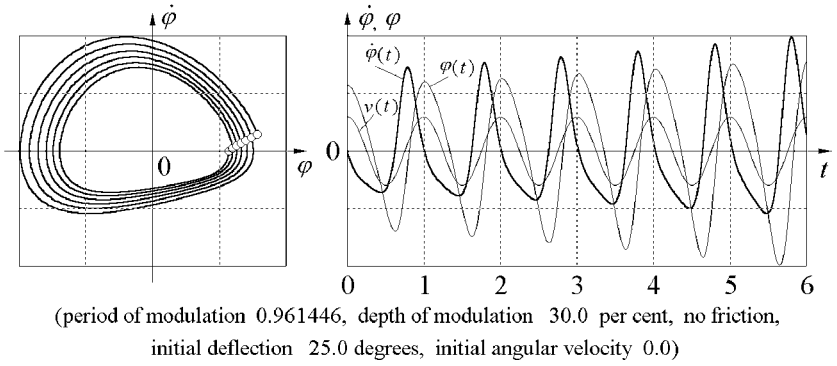

Figure 7. The phase trajectory of oscillations in conditions of the second parametric resonance (left) and graphs of the angular velocity and of the radial velocity of the weights (right).

For arbitrary values of the modulation depth m, the calculated boundaries of the principal instability interval are shown by the first 'tongue' of the T–m diagram in figure 5.

6. Resonance of the second order

In contrast to the principal resonance, for which the energy supply due to the parameter modulation occurs even if we assume the torsional oscillations to be purely sinusoidal (see equation (7)), for the second resonance a positive net energy delivery is possible only by virtue of the asymmetric distortions in the shape of the oscillations. These distortions are clearly seen in figure 7. They provide the motion of the weights towards the axis of rotation ($v > 0$) to happen on average at a greater (in magnitude) angular velocity $\dot\varphi$ than the backward motion. The distortions can be described by the second harmonic component (frequency 2ω), whose contribution is proportional to the depth of modulation m. Hence the amount of energy delivered by modulation in conditions of the second parametric resonance is proportional not to m (as at the principal resonance, see equation (10)), but only to m^2.

In order to find the boundaries of the second interval of parametric instability with $n = 2$, for which $\omega \approx \omega_0$ (or $T \approx T_0$), we look for a periodic solution of equation (18) near the value $\omega = \omega_0$. Considering terms up to the second order in the modulation depth m, we should include in this approximate solution the sinusoidal oscillations with the fundamental frequency[2] $\omega = \omega_0 + \varepsilon$ (the frequency of modulation) and the second harmonic with the frequency 2ω:

$$\varphi(t) = C_2 \cos\omega t + S_2 \sin\omega t + C_4 \cos 2\omega t + S_4 \sin 2\omega t. \tag{26}$$

An example of such stationary oscillations is shown in figure 8.

Substituting $\varphi(t)$ into equation (18), we transform there the products of sine and cosine functions into sums, keeping the terms with the frequencies ω and 2ω. Thus, for the coefficients

[2] However, it may be convenient to consider the fundamental frequency of parametrically excited stationary oscillations to be always equal to one-half of the frequency of modulation. Then the spectrum of oscillations in the case of resonance of an odd order includes only odd harmonics. The spectrum of stationary oscillations for resonance of an even order includes only even harmonics (the amplitude of the fundamental harmonic being zero). We follow this convention introducing relevant notation for the coefficients of harmonics in equation (26).

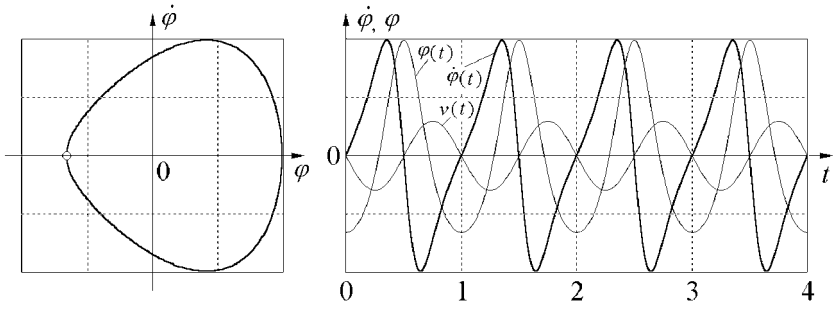

(period of modulation 0.950234, depth of modulation 30.0 per cent, no friction, initial deflection −90.0 degrees, initial angular velocity 0.0)

Figure 8. The phase trajectory of stationary oscillations occurring at the left boundary of the second instability interval (left) and graphs of the angular velocity and of the radial velocity of the weights (right).

C_2, S_2, and C_4, S_4 we obtain the following system of homogeneous equations:

$$\begin{aligned}
&\left(1-\frac{\omega_0^2}{\omega^2}\right)C_2+\frac{3}{4}m^2C_2+2mS_4-\frac{2\gamma}{\omega_0}S_2=0,\\
&\left(1-\frac{\omega_0^2}{\omega^2}\right)S_2+\frac{1}{4}m^2S_2+2mC_4+\frac{2\gamma}{\omega_0}C_2=0,\\
&3C_4-2mS_2=0,\qquad 3S_4+2mC_2=0.
\end{aligned}\tag{27}$$

The last two equations of the system give us the expressions for the amplitudes C_4 and S_4 of the second harmonic in $\varphi(t)$ in terms of the depth of modulation m and the amplitudes C_2 and S_2 of the principal harmonic:

$$C_4=\tfrac{2}{3}mS_2,\qquad S_4=-\tfrac{2}{3}mC_2.\tag{28}$$

These relations essentially mean that the amplitude of the second harmonic in the stationary oscillations equals $\frac{2}{3}m$ times the amplitude of the principal harmonic. The ratio of the amplitudes of these harmonics is the same for both boundaries of the interval. However, for the left and right boundaries these harmonics add with different relative phases, creating different shapes of resulting oscillations. Graphs of oscillations occurring at the right boundary of the second instability interval are shown in figure 9.

Substituting C_4 and S_4 from equation (28) into the first two equations of the system, equation (27), and taking into account that $\omega^2=(\omega_0+\varepsilon)^2\approx\omega_0^2+2\omega_0\varepsilon$, we obtain the system of two homogeneous equations for C_2 and S_2:

$$\begin{aligned}
&\left(\frac{2\varepsilon}{\omega_0}-\frac{7}{12}m^2\right)C_2-\frac{2\gamma}{\omega_0}S_2=0,\\
&\frac{2\gamma}{\omega_0}C_2+\left(\frac{2\varepsilon}{\omega_0}-\frac{13}{12}m^2\right)S_2=0.
\end{aligned}\tag{29}$$

Nontrivial solution to this system exists if its determinant equals zero. This condition determines the values of $\varepsilon=\omega-\omega_0$ which correspond to the boundaries $\omega_\pm$ of the second interval of instability:

$$\omega_\pm=\left(1+\tfrac{5}{12}m^2\pm\tfrac{1}{8}\sqrt{m^4-(4/Q)^2}\right)\omega_0.\tag{30}$$

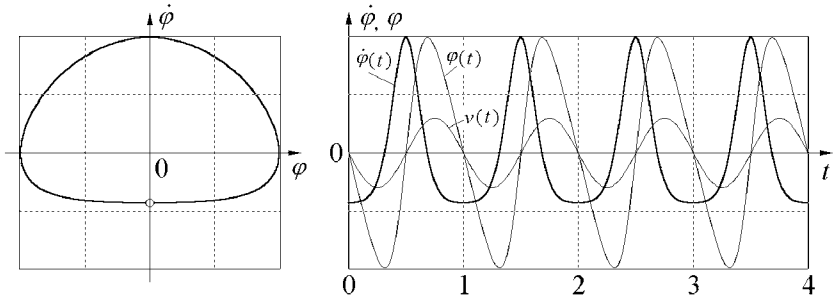

(period of modulation 0.972658, depth of modulation 30.0 per cent, no friction, initial deflection 0.0 degrees, initial angular velocity −1.0)

Figure 9. The phase trajectory of stationary oscillations occurring at the right boundary of the second instability interval (left) and graphs of the angular velocity and of the radial velocity of the weights (right).

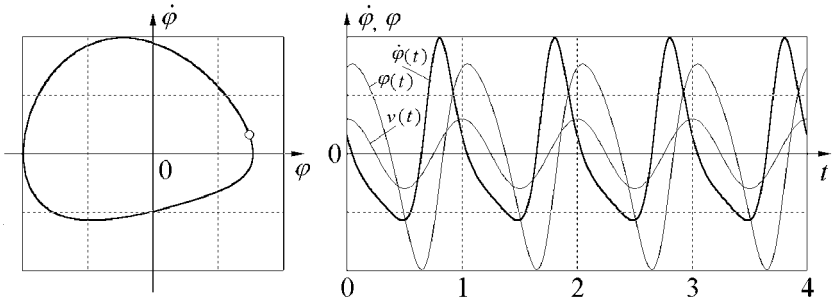

(period of modulation 0.964, depth of modulation 30.0 per cent, quality 48.0, initial deflection 30.0 degrees, initial angular velocity 0.15)

Figure 10. The phase trajectory of stationary oscillations occurring at the threshold of the second instability interval (left) and the graphs of the angular velocity and of the radial velocity of the weights (right).

We note that even the lower boundary is displaced to a higher frequency from the value ω_0. The boundaries of the interval merge at the threshold. From equation (30), we find the threshold conditions for the second parametric resonance:

$$m_{\min} = \frac{2}{\sqrt{Q}}, \qquad Q_{\min} = \frac{4}{m^2}, \qquad \omega_{\text{res}} = \left(1 + \frac{5}{12}m^2\right)\omega_0. \tag{31}$$

Stationary oscillations occurring at the threshold of the second parametric resonance are illustrated in figure 10.

In order to observe the mode of parametric regeneration (stationary oscillations at the threshold of the second parametric resonance) for a given modulation depth m in the simulation experiment, we should choose the period of modulation and the quality factor according to equation (31), and set the initial conditions properly. For the threshold equations (29) give $S_2 = C_2$. Therefore,

$$\varphi(0) = C_2\left(1 + \tfrac{2}{3}m\right), \qquad \dot\varphi(0) = \omega_0 C_2\left(1 - \tfrac{4}{3}m\right). \tag{32}$$

To produce stationary oscillations, we can choose arbitrarily an initial angular displacement $\varphi(0)$, and enter an initial angular velocity $\dot\varphi(0) = \omega_0\varphi(0)(1 - 2m)$, as follows

from equation (32). Or, equivalently, we can choose an arbitrary initial velocity $\dot{\varphi}(0)$, and enter an initial displacement $\varphi(0) = \dot{\varphi}(0)(1 + 2m)/\omega_0$.

In the absence of friction, the width of the second interval of instability is proportional to the square of the depth of modulation: $\omega_+ - \omega_- = m^2\omega_0/4$. Equation (30) gives the following boundaries of the interval for zero friction:

$$\omega_+ = \left(1 + \tfrac{13}{24}m^2\right)\omega_0, \qquad \omega_- = \left(1 + \tfrac{7}{24}m^2\right)\omega_0. \tag{33}$$

To find the frequencies corresponding to these boundaries with a greater precision, we should include more harmonics into the trial function $\varphi(t)$, equation (26). In the absence of friction it is more convenient to assume that the motion of the weights along the rod is described in equation (2) by $l(t) = l_0(1 + m\cos\omega t)$ instead of the sine function. In this case, the stationary oscillations at the left boundary of the interval include only harmonics of the cosine type, and at the right boundary—of the sine type.

The final (rather complicated) expressions for the periods of modulation and for the relative contributions of high harmonics at the boundaries of the instability interval show a very good agreement with the simulations. Below we cite the calculated values for the modulation depth $m = 0.3$ (30%). The corresponding experimental values are shown in the parentheses:

- Left (cosine-type) boundary: period $T/T_0 = 0.9502$ (0.9502); $C_4/C_2 = -0.203$ (-0.202); $C_6/C_2 = 0.038$ (0.039).
- Right (sine-type) boundary: period $T/T_0 = 0.9727$ (0.9727); $S_4/S_2 = -0.207$ (-0.207); $S_6/S_2 = 0.039$ (0.039).

For arbitrary values of the modulation depth m the calculated boundaries of this instability interval are shown by the second 'tongue' of the T–m diagram in figure 5.

In order to observe stationary oscillations in the simulation experiment for the case when friction is zero, we should choose the period of modulation corresponding to one of these boundaries, and set the initial conditions properly. If $l(t) = l_0(1 + m\cos\omega t)$, for the left boundary we can choose arbitrarily an initial angular displacement $\varphi(0)$ and zero initial angular velocity. For the right boundary, vice versa, we choose arbitrarily an initial angular velocity $\dot{\varphi}(0)$ and zero initial displacement.

7. Resonances of the third and higher orders

Oscillations that occur in conditions of any parametric resonance have a mean period which is rather close to the natural one. To compensate for or to overcome the frictional losses by modulation of the moment of inertia, two cycles of modulation must be complete during an integer number n of (almost natural) oscillations of the rotor: $2T \approx nT_0$. The width ΔT of high order resonance bands (of the intervals of parametric instability) diminishes very quickly as the order n of resonance is increased—as m^n. The index α of the rate of the amplitude growth also diminishes as fast as ΔT does with the increase in n. Both these properties make an experimental observation of parametric resonances of high orders ($n > 1$) at moderate values of m very difficult. High-order instability intervals disappear in the presence of very small friction.

Stationary oscillations at the threshold of parametric resonance of the third order are shown in figure 11.

In order to find the boundaries of the third instability interval in the absence of friction, we assume that the weights move according to $l(t) = l_0(1 + m\cos\omega t)$, and use the trial function $\varphi(t)$ that includes the fundamental harmonic of the frequency $\frac{1}{2}\omega$ and several high odd-numbered harmonics of frequencies $\frac{3}{2}\omega$, $\frac{5}{2}\omega$, ... Stationary oscillations at the left boundary

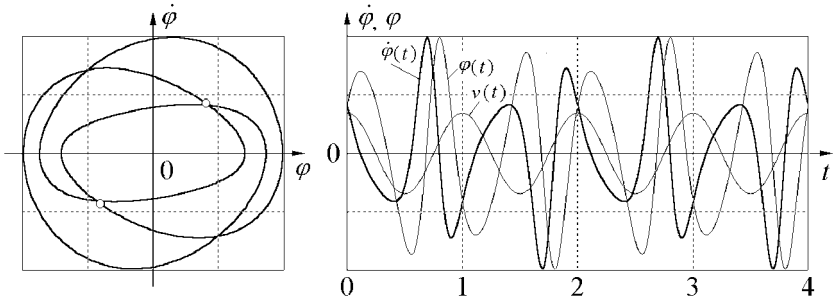

(period of modulation 1.41157, depth of modulation 35.0 per cent, quality 300.0, initial deflection 16.9 degrees, initial angular velocity 0.46)

Figure 11. The phase trajectory and the time-dependent graphs of stationary oscillations at the threshold of the third parametric resonance.

comprise only harmonics of cosine type, and at the right boundary—of sine type. After substituting the trial function into the differential equation

$$\frac{\mathrm{d}}{\mathrm{d}t}\left[(1+m\cos\omega t)^2\frac{\mathrm{d}}{\mathrm{d}t}\varphi\right]+\omega_0^2\varphi=0, \tag{34}$$

we equate to zero the coefficients of cosine (or sine) functions with frequencies $\frac{1}{2}\omega$, $\frac{3}{2}\omega$, $\frac{5}{2}\omega,\ldots$, and thus get a system of homogeneous equations for the coefficients $C_1, C_3, \ldots$ (or $S_1, S_3, \ldots$) of harmonic components in the trial function. The condition of existence of a nontrivial solution to this system yields an equation for the desired boundaries. This equation is the same as for the boundaries of the principal instability interval, but this time we look for its approximate solution in the vicinity of $\frac{3}{2}T_0$ (instead of $\frac{1}{2}T_0$). The third harmonic component (frequency $\frac{3}{2}\omega$) dominates the spectrum.

To increase precision, more harmonics should be included in the trial function $\varphi(t)$. We cite below the values of the period and of the relative contributions of different harmonics at stationary oscillations for the modulation depth $m = 0.3$, obtained by a calculation in which harmonics up to 13th order were included. (We use the *Mathematica*-4 package by Wolfram Research Inc.) The corresponding experimental values are shown in parentheses:

- Left (cosine-type) boundary: period $T/T_0 = 1.4336$ (1.4336);
  $C_1/C_3 = 0.107$ (0.110); $C_5/C_3 = -0.289$ (-0.288); $C_7/C_3 = 0.065$ (0.067).
- Right (sine-type) boundary: period $T/T_0 = 1.4369$ (1.4369);
  $S_1/S_3 = 0.135$ (0.136); $S_5/S_3 = -0.291$ (-0.292); $S_7/S_3 = 0.066$ (0.066).

Stationary oscillations at the boundaries of the third interval of parametric instability are shown in figure 12.

Similar calculations allow us to find the periods of modulation at which resonances of higher orders occur. The corresponding ranges of parametric instability are very narrow, that is, both their boundaries very nearly coincide. We cite below the calculated values of the modulation periods and the spectral composition of stationary oscillations for the boundaries of the fourth and fifth resonances (at $m = 0.3$):

- Left (cosine-type) boundary of fourth resonance: period $T/T_0 = 1.9107$ (1.9107); $C_2/C_4 = 0.219$ (0.220); $C_6/C_4 = -0.377$ (-0.374); $C_8/C_4 = 0.100$ (0.102); $C_{10}/C_4 = -0.023$ (-0.021).

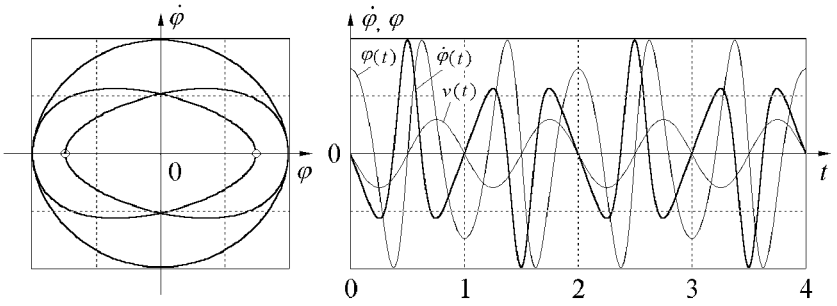

(period of modulation 1.433648, depth of modulation 30.0 per cent, no friction, initial deflection 90.0 degrees, initial angular velocity 0.0)

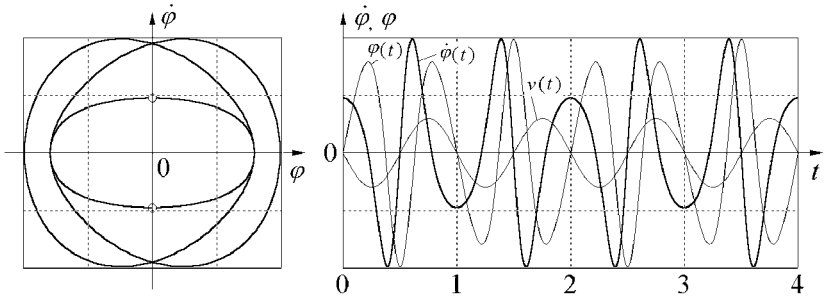

(period of modulation 1.436914, depth of modulation 30.0 per cent, no friction, initial deflection 0.0 degrees, initial angular velocity 1.0)

Figure 12. The phase trajectories and the time-dependent graphs of stationary oscillations at the boundaries of the third interval of parametric instability.

- Right (sine-type) boundary of fourth resonance: period $T/T_0 = 1.9112$ (1.9112); $S_2/S_4 = 0.222$ (0.222); $S_6/S_4 = -0.377$ (-0.377); $S_8/S_4 = 0.100$ (0.100); $S_{10}/S_4 = -0.023$ (-0.023).
- Left (cosine-type) boundary of fifth resonance: period $T/T_0 = 2.3872$ (2.3872); $C_1/C_5 = 0.017$ (0.019); $C_3/C_5 = 0.319$ (0.321); $C_7/C_5 = -0.459$ (-0.466); $C_9/C_5 = 0.124$ (0.146).
- Right (sine-type) boundary of fifth resonance: period $T/T_0 = 2.3873$ (2.3873); $S_1/S_5 = 0.020$ (0.020); $S_3/S_5 = 0.321$ (0.321); $S_7/S_5 = -0.468$ (-0.468); $S_9/S_5 = 0.142$ (0.144).

The spectral composition, phase trajectories and time-dependent graphs of stationary oscillations at the boundaries of the fourth and fifth intervals of parametric instability are shown in figures 13 and 14, respectively.

Almost exact coincidence of both boundaries for the high-order intervals means that at the period of modulation corresponding to one of the intervals, we can actually observe (in the absence of friction) not a resonant growth but rather stationary oscillations of a constant (arbitrarily large) amplitude. From the graphs in figures 13 and 14 we can conclude that at exact tuning to n-order resonance, the oscillator completes just the whole number n of natural oscillations (of varying period and amplitude) exactly during two cycles of modulation. The process is periodic at arbitrary initial conditions, in contrast to the boundaries of low orders, for which special initial conditions are required to provide periodic oscillations.

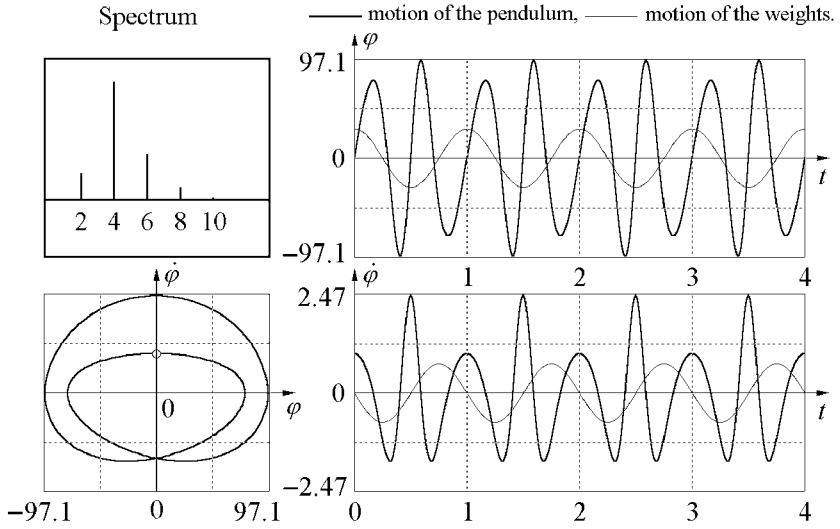

Figure 13. The spectrum, phase trajectory and time-dependent graphs of stationary oscillations at the right boundary of the fourth interval of parametric instability.

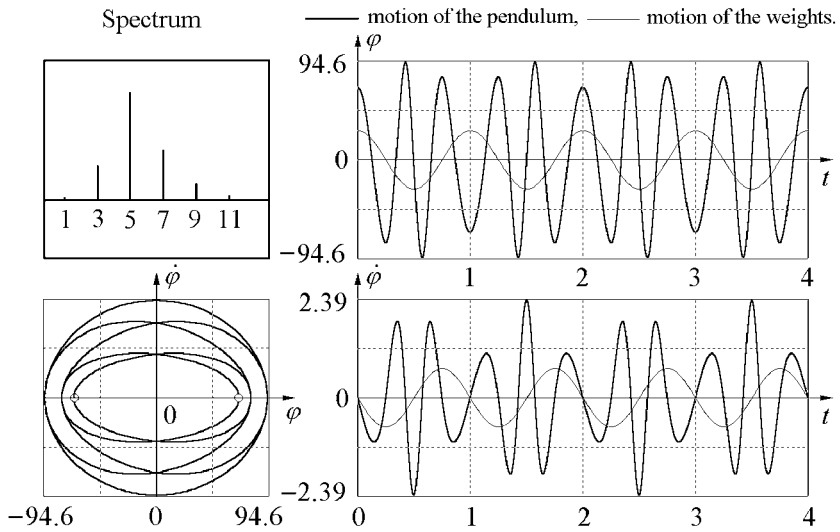

Figure 14. The spectrum, phase trajectory and time-dependent graphs of stationary oscillations at the left boundary of the fifth interval of parametric instability.

This behaviour can be explained in terms of the familiar phenomenon of frequency modulation. For parametric resonances of high orders, the weights move along the rod rather slowly compared to the natural torsional oscillations of the rotor ($T \gg T_0$). A slow periodic variation of the moment of inertia means that the current natural frequency of the oscillator is

slowly modulated. We see clearly in figures 13 and 14 how oscillations slow down when the weights are moved towards the ends of the rotor, and vice versa. Hence we can consider the motion of the rotor in conditions of high-order parametric resonance as a frequency modulated oscillation, in which the natural oscillation—the dominating harmonic component—plays the role of a carrier.

The spectral composition shown in figures 13 and 14 gives convincing evidence of this interpretation. The harmonic component with the frequency $n\omega/2 \approx \omega_0$ has the greatest amplitude (the carrier). The coefficients C_{n-2} and C_{n+2} of lateral spectral components with frequencies $(n\omega/2) \pm \omega$ have opposite signs and (for $n \gg 1$) are nearly equal in magnitude. This spectrum is characteristic of the frequency modulation.

8. Concluding remarks

We have developed in this paper a theoretical approach to the phenomenon of parametric resonance complemented by a computerized experimental investigation. A simple mathematical model of the physical system (based on a linear differential equation) is used. The model allows a complete quantitative description of the parametric excitation, which can be verified by the simulations [3]. The visualization of motion, along with the plot of the graphs of different variables and phase trajectories, makes the simulation experiments very convincing and comprehensible. This investigation provides a good background for the study of more complicated nonlinear parametric systems such as a pendulum whose length is periodically changed (a model of the playground swing), or a pendulum with the suspension point driven periodically in the vertical direction [2].

References

[1] Case W 1996 The pumping of a swing from the standing position *Am. J. Phys.* **64** 215–20
[2] Butikov E I 2001 On the dynamic stabilization of an inverted pendulum *Am. J. Phys.* **69** 755–68
[3] Butikov E I 1996 Educational software package *Physics of Oscillations* ed J S Risley and R W Brehme (New York: AIP)
[4] Phelps F M and Hunter J H Jr 1965 An analytic solution of the inverted pendulum *Am. J. Phys.* **33** 285–95
Phelps F M and Hunter J H Jr 1966 An analytic solution of the inverted pendulum *Am. J. Phys.* **34** 215–20, 533–35
[5] Landau L D and Lifschitz E M 1958 *Mechanics* (Moscow: Fizmatlit)
Landau L D and Lifschitz E M 1976 *Mechanics* (New York: Pergamon) pp 93–5 (Engl. Transl.)